Research article JHEP|Reports

Mitosis of hepatitis B virus-infected cells *in vitro* results in uninfected daughter cells

Authors

Thomas Tu, Benno Zehnder, Jochen M. Wettengel, Henrik Zhang, Sally Coulter, Vikki Ho, Mark W. Douglas, Ulrike Protzer, Jacob George, Stephan Urban

Correspondence

t.tu@sydney.edu.au, thomas.tu.phd@gmail.com (T. Tu).

Graphical abstract

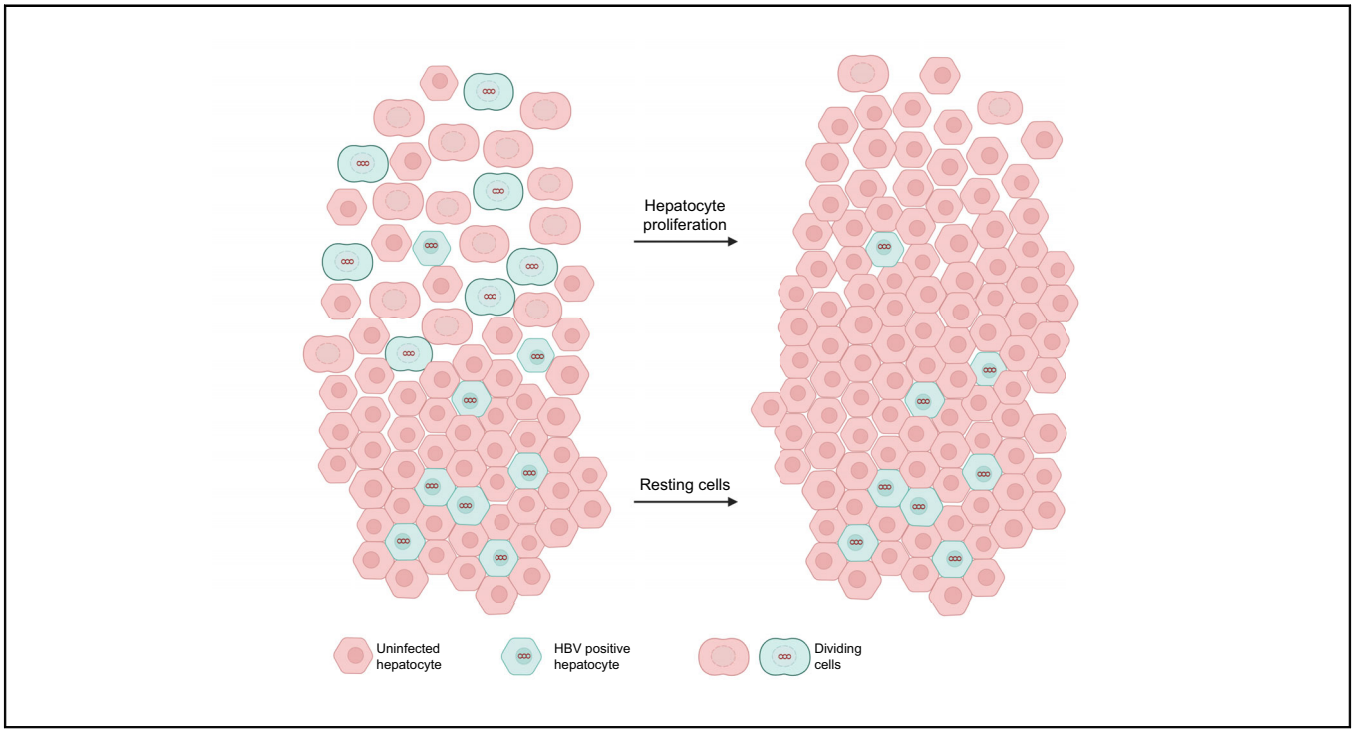

Highlights

- HBV persists over decades in the liver, leading to chronic inflammation and serious liver disease.
- Controversy exists over the fate of viral DNA after cell mitosis, which is crucial to understanding viral persistence.
- We find here that 2 completely uninfected daughter cells are generated when infected cells undergo mitosis.
- Our results suggest that therapies that induce turnover of infected cells could facilitate the clearance of chronic HBV infection.

Lay summary

Chronic hepatitis B affects 300 million people (killing 884,000 per year) and is incurable. To cure it, we need to clear the HBV genome from the liver. In this study, we looked at how the virus behaves after a cell divides. We found that it completely clears the virus, making 2 new uninfected cells. Our work informs new approaches to develop cures for chronic hepatitis B infections.

https://doi.org/10.1016/j.jhepr.2022.100514

Research article

JHEP|Reports

Mitosis of hepatitis B virus-infected cells *in vitro* results in uninfected daughter cells

Thomas Tu,[1,2,*] Benno Zehnder,[3] Jochen M. Wettengel,[4,5] Henrik Zhang,[1] Sally Coulter,[1] Vikki Ho,[1] Mark W. Douglas,[1,2] Ulrike Protzer,[4,5] Jacob George,[1,†] Stephan Urban[3,6,†]

[1]*Storr Liver Centre, Westmead Clinical School and Westmead Institute for Medical Research, Faculty of Medicine and Health, The University of Sydney, Westmead, NSW, Australia;* [2]*Sydney Institute for Infectious Diseases, University of Sydney at Westmead Hospital, Westmead, NSW, Australia;* [3]*Department of Infectious Diseases, Molecular Virology, University Hospital Heidelberg, Heidelberg, Germany;* [4]*Institute of Virology, Technische Universität München/Helmholtz Zentrum München, Munich, Germany;* [5]*German Center for Infection Research (DZIF), Munich Partner Site, Munich, Germany;* [6]*German Center for Infection Research (DZIF), Heidelberg Partner Site, Heidelberg, Germany*

JHEP Reports **2022.** https://doi.org/10.1016/j.jhepr.2022.100514

Background & Aims: The chronicity of HBV (and resultant liver disease) is determined by intrahepatic persistence of the HBV covalently closed circular DNA (cccDNA), an episomal form that encodes all viral transcripts. Therefore, cccDNA is a key target for new treatments, with the ultimate therapeutic aim being its complete elimination. Although established cccDNA molecules are known to be stable in resting hepatocytes, we aimed to understand their fate in dividing cells using *in vitro* models.
Methods: We infected HepG2-NTCP and HepaRG-NTCP cells with HBV and induced mitosis by passaging cells. We measured cccDNA copy number (by precise PCR assays) and HBV-expressing cells (by immunofluorescence) with wild-type HBV. We used reporter viruses expressing luciferase or RFP to track number of HBV-expressing cells over time after mitosis induction using luciferase assays and live imaging, respectively.
Results: In all cases, we observed dramatic reductions in cccDNA levels, HBV-positive cell numbers, and cccDNA-dependent protein expression after each round of cell mitosis. The rates of reduction were highly consistent with mathematical models of a complete cccDNA loss in (as opposed to dilution into) daughter cells.
Conclusions: Our results are concordant with previous animal models of HBV infection and show that HBV persistence can be efficiently overcome by inducing cell mitosis. These results support therapeutic approaches that induce liver turnover (*e.g.* immune modulators) in addition to direct-acting antiviral therapies to achieve hepatitis B cure.
Lay summary: Chronic hepatitis B affects 300 million people (killing 884,000 per year) and is incurable. To cure it, we need to clear the HBV genome from the liver. In this study, we looked at how the virus behaves after a cell divides. We found that it completely clears the virus, making 2 new uninfected cells. Our work informs new approaches to develop cures for chronic hepatitis B infections.

Introduction

HBV is an enveloped, partially double-stranded DNA virus and the prototypic member of the *Hepadnaviridae*. Chronic infection with HBV confers a high risk of developing liver cirrhosis and hepatocellular carcinoma, causing ~600,000 deaths annually.[1] HBV is not cytopathic; instead, liver injury is driven by virus-induced inflammatory immune responses that are insufficient to eradicate infected hepatocytes. Thus, chronic HBV infection is often a life-long and incurable condition, which in turn drives other personal impacts (*e.g.* anxiety about disease progression, stigma and discrimination, and long-term healthcare costs).[2]

Persistence of covalently closed circular viral DNA (cccDNA) in the hepatocyte is the critical determinant of chronic hepatitis B infection. cccDNA is an episomal plasmid-like 'mini-chromosome' that acts as the transcriptional template for HBV mRNAs and the pregenomic RNA and is therefore necessary for viral replication. However, the host immune responses are usually suboptimal and cannot fully eliminate all cccDNA-containing hepatocytes. Given its supercoiled structure and complexing with cellular histones, cccDNA is stable within an infected hepatocyte (likely for its entire lifetime),[3,4] although some studies have suggested partial non-cytolytic clearance.[5–7] Additional routes of cccDNA elimination from the liver are immune-mediated killing of cccDNA-containing hepatocytes and possibly loss following mitosis.[8] Understanding the mechanisms behind the elimination of cccDNA will greatly aid in developing therapeutics to overcome chronic HBV infections.

Elimination of cccDNA in infected hepatocytes would result in a cure of chronic HBV,[9] which cannot be efficiently achieved by current treatment options. Clearance of cccDNA would allow

Keywords: Covalently closed circular DNA; Hepatitis B virus; Viral persistence; cinqPCR.
Received 13 April 2022; accepted 16 May 2022; available online 15 June 2022
† Equal contribution.
* Corresponding author. Address: Storr Liver Centre, Westmead Clinical School and Westmead Institute for Medical Research, Faculty of Medicine and Health, The University of Sydney, Westmead, NSW 2145, Australia. Tel.: +612-8627-3912
E-mail addresses: t.tu@sydney.edu.au, thomas.tu.phd@gmail.com (T. Tu).

cessation of therapy without viral rebound, thereby slowing liver pathogenesis. Mathematical models predict that various independent parameters (including the cccDNA copy number per cell, its rate of degradation, and its stability in resting and replicating cells) profoundly affect the dynamics of cccDNA clearance.[10,11] These dynamics are not fully resolved, as there is controversy as to whether mitosis of an infected cell results in 2 uninfected daughter cells[8,12] or if cccDNA survives and is diluted amongst the daughter cells.[4,10,13,14]

The reduction of cccDNA levels with mitosis critically determines the optimal cure strategy: for example, if the cccDNA pool of an infected hepatocyte is lost within 1 round of mitosis, then activation of antiviral immunity or other methods to induce turnover of infected cells become an attractive option for treatment. In contrast, if cccDNA survives mitosis, greater emphasis on cccDNA degrading pathways (*e.g.* CRISPR-Cas9) or direct killing of infected cells (*e.g.* CAR-T cell technology) may be of higher priority. Given the central importance of cccDNA reduction for how the field should proceed with therapeutic cures of chronic hepatitis B, we aimed to clarify the fate of cccDNA after cell mitosis.

We used a novel **c**cccDNA **in**version **q**uantitative (cinq)PCR assay[15,16] to precisely quantify cccDNA levels. We find that cccDNA levels undergo an ~5-fold decrease after each round of mitosis, which is the exact rate predicted by mathematical models assuming a complete loss of cccDNA in daughter cells. Evidence from orthogonal approaches using reporter HBVs was consistent with this model, down to the level of a single cell. Thus, we unequivocally show that liver turnover is an efficient mechanism to clear HBV cccDNA, which informs future therapeutic approaches to the cure of chronic hepatitis B.

Materials and methods

Production of HBV inoculum

For wild-type (WT) HBV, virus stocks were purified from the supernatant of HepAD38 cells by heparin affinity chromatography, as previously described.[17,18] For HBV core protein (HBc)-deficient HBV (and associated WT control), the virus was further concentrated using a 100-kDa Amicon Ultra-15 centrifugal filter (UFC910024, Merck) from the supernatant of Huh7 cells transfected with plasmid constructs containing an over-length HBV genome (coding for HBV pgRNA and HBV proteins) and a complementing HBc overexpression plasmid (encoding HBc under a cytomegalovirus promoter), as previously described.[16]

A reporter HBV (rHBV) encoding secreted Gaussia luciferase (GLuc) under a transcriptionally strong transthyretin (TTR) promoter (rHBV-TTR-GLuc) and an rHBV that expresses turbo-RFP (tRFP) under the control of a TTR promoter (rHBV-TTR-tRFP; hereafter referred to as 'tRFP-HBV') were generated in HepG2 cell lines that were stably cotransduced with a plasmid expressing HBV Polymerase, Surface Proteins and X, and a recombinant HBV genome construct encoding HBV pgRNA with the HBsAg open reading frame (ORF) replaced by an ORF encoding either tRFP or GLuc under a TTR promoter (as previously described[19]). Reporter virus stocks were purified by heparin affinity chromatography and sucrose gradient ultracentrifugation of the supernatant of these cells, as previously described.[20]

Cell culture and HBV infection

HepaRG-NTCP (differentiated as previously described[21]) and HepG2-NTCP cells[22] were used for *in vitro* infection. HepaRG-NTCP cells were cultivated in William's E media supplemented with 1.5% DMSO.[21,23] HepG2-NTCP cells were maintained in DMSO-free DMEM.[22] HepG2-NTCP or differentiated HepaRG-NTCP cells were seeded in 12-well plates and infected with HBV at up to 500 VGE/cell in 250 μl of culture media supplemented with 4% v/v polyethylene glycol 8000 (Sigma Aldrich, St. Louis, MO, USA) and 1.5% v/v (for HepaRG-NTCP) or 2.5% v/v DMSO (for HepG2-NTCP). Cells were washed twice with 1× PBS at 24-h post-infection. At 3, 6, 9, and 12 dpi, cells were trypsinised, and the cell suspension was split in half: one half reseeded in a new 12-well plate and the other frozen at -20°C for DNA extraction and cinqPCR analysis. In an alternate experimental setup (setup 2), instead of harvesting the second half of the cell suspension for DNA extraction, they were reseeded in a new 12-well plate but did not undergo further splitting, and all cells were harvested at 12 dpi.

Detection of HBc-positive cells by immunofluorescence

Cells were seeded onto 13-mm-diameter glass coverslips in 24-well plates. At cell harvest, culture media were aspirated from the cells, which were then washed with 1 ml 1× PBS and fixed with 300 μl 4% w/v formaldehyde for 20 min at room temperature. Cells were permeabilised with 0.25% v/v Triton-X in 1× PBS for 20 min at room temperature. HBV core antigen was then detected using a 1:3,000 dilution of polyclonal rabbit anti-HBc antibody (B0586, Dako, Denmark)[23] overnight at 4°C. After washing with 1× PBS, 1:500 AF545-conjugated goat anti-rabbit secondary antibody (A-11010, Invitrogen) and 2 μg/ml Hoechst 33342 (H1399, Invitrogen) in 1 ml PBS was overlaid on the cells, which were incubated in the dark at room temperature for 1 h. Fluorescence microscopy images were taken at 40× magnification with appropriate DAPI and Texas Red filter sets. For each sample, an area the size of 5 random fields of view were acquired using a BX53/DP80 Fluorescence Microscope (Olympus, Shinjuku City, Tokyo, Japan) and cellSens Standard software (Olympus). Images were edited with ImageJ imaging software[24] and quantified using Ilastik image classification, segmentation, and analysis software (https://www.ilastik.org/, version 1.3.3).[25]

Quantification of total HBV DNA, cccDNA, and cellular genome copy numbers by cinqPCR

The cinqPCR protocol was carried out as previously described.[15,16,26] Total cellular DNA was extracted from harvested cells using a NucleoSpin® Tissue kit (740952, Macherey-Nagel, Düren, Germany) as per the manufacturer's instructions and eluted in 50 μl of elution buffer. Then, 10 μl of the DNA extract was digested in a 20 μl restriction digestion reaction containing 1 × CutSmart buffer (B7204, New England Biolabs [NEB], Ipswich, MA, USA), 7.5 U $RecJ_f$ (M0264, NEB), and 10 U *Hha*I (R0139, NEB). The combined restriction digestion and exonuclease reaction was incubated for 4 rounds of a 15-min interval at 37°C, followed by a 15-min interval at 42°C. The enzymes were then heat-inactivated at 80°C for 20 min. To circularise the digested fragments, a 10 μl solution containing 500 U of T4 DNA Ligase (M0202, NEB) in 1× CutSmart buffer and 3 mMol molecular-grade ATP (P0756, NEB) was added to the reaction. The reaction was incubated at 16°C for 2 h, followed by an inactivation step of 80°C for 20 min and holding at 4°C. A final linearisation step was performed by adding 5 μl solution containing 10 U *Xba*I (R0145, NEB) in 1× CutSmart buffer and incubating at 37°C for 2 h and 80°C for 20 min and then storing at 4°C until further use.

For digital droplet (dd)PCR analysis, 2 μl of the inverted product was put in a 20 μl ddPCR reaction composed of 1× ddPCR Supermix for Probes (1863024, Bio-Rad, Hercules, CA, USA), 1× VIC-labelled TaqMan™ Copy Number Reference Assay for the human RNase P gene (4403328, Applied Biosystems, Foster City, CA, USA), and 150 pMol of each HBV DNA-specific primer and probe (all synthesised by Eurofins Scientific, Luxembourg). The forward, reverse, and probe sequences for the inverted HBV cccDNA fragment were 5′-CACTCTATGGAAGGCGGGTA-3′, 5′-ATAAGGGTCGATGTCCATGC-3′, and 5′-FAM-AACACA-TAGCGCACCAGCA-BHQ1-3′, respectively. The forward, reverse, and probe sequences to detect total HBV DNA copies were 5′-GTGTCTGCGGCGTTTTATCA-3′, 5′-GACAAACGGGCAACATACCTT-3′, and 5′-FAM-TGAGGCATAGCAGCAGGATG-BHQ1-3′, respectively. Droplets were generated according to the manufacturer's protocol using a QX200 Droplet Generator (Bio-Rad). Intra-droplet PCR was carried out using the following protocol: an initial 10-min denaturation, enzyme activation, and droplet stabilisation step at 95°C, followed by 40 cycles of a 10-s denaturation step at 95°C, a 15-s annealing step at 54°C, and a 20-s elongation step at 68°C, finished with a 10-min enzyme deactivation step at 95°C. Products were then stored at 12°C until droplet reading using a QX200 Droplet Reader (Bio-Rad), quantification using FAM and VIC channels, and data analysis using QuantaSoft (Bio-Rad).

Quantifying cccDNA-dependent protein expression by measuring luciferase activity

HepG2-NTCP cells were infected with ∼500 VGE/cell of rHBV-TTR-GLuc in 24-well plates and serially split over 21 days. Supernatant was collected every 3 days, centrifuged at 500× *g* to remove cell debris, and then stored at -20°C. Pierce™ Gaussia Luciferase Flash Assay Kit (16158, ThermoFisher Scientific) was used to measure luciferase activity, per the manufacturer's instructions. In brief, 10 μl of cell supernatant was added to a black opaque 96-well plate (6005270, PerkinElmer, Waltham, MA, USA). In addition, 50 μl of working solution (1× coelenterazine in the Gaussia Flash Assay Buffer) was added and mixed using a pipette. Luminescence was then immediately read with a SpectraMax iD5 Plate Reader (Molecular Devices, San Jose, CA, USA).

Detection of HBc-positive cells by live imaging microscopy

HepG2-NTCP cells were infected as described above with ∼500 VGE/cell of tRFP-HBV in a 24-well plate. At 3 days post-infection (dpi), cells were seeded into a Nunc Lab-Tek™ 8-well chamber (ThermoFisher Scientific, 177402PK) slides at a concentration of ∼100,000 cells per cm^2 in 400 μl DMSO-free DMEM to stimulate cell mitosis. After allowing cells to attach for 8 h post-seeding, sliders were transferred into a humidity-, heat-, and CO_2-controlled chamber connected to a Zeiss AxioVert 200M (Carl Zeiss Microscopy GmbH, Jena, Germany). RFP-positive cells were then visualised by phase microscopy and fluorescence using a Texas Red filter set (excitation: 560/40 nm; emission: 630/75 nm) with a 40× objective lens. Images were acquired every 15 min from 10 fields of view per slide for 36 h. Each field of view was then exposed for a total of 10 min of 560/40-nm light. After a recovery period of 4 h, images from the same fields of view were then acquired exactly as described above with identical settings. Images were acquired using Zeiss Zen Pro imaging software (Carl Zeiss Microscopy GmbH) and edited using ImageJ imaging software.[24]

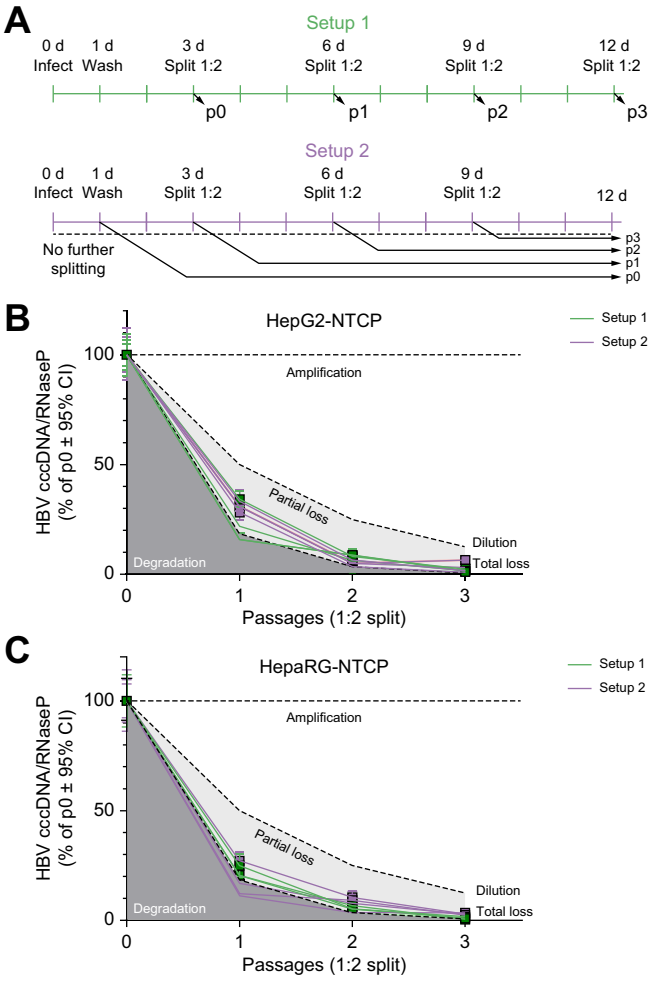

Fig. 1. cccDNA levels are profoundly reduced after rounds of cell mitosis in HepG2-NTCP and HepaRG-NTCP cells. (A) Two experimental setups were used to study the fate of cccDNA following cell mitosis with the main difference being whether cells left over from the splitting were immediately lysed (setup 1, green) or cultured until 12 dpi before DNA was extracted and analysed by cinqPCR (setup 2, purple). (B and C) Dilution and complete loss models (top and bottom dashed lines, respectively) predict different levels of cccDNA decrease (50 and 18.4% of the presplit value per passage, respectively). The area between these 2 models (light grey) represents a model where there is partial loss of cccDNA during mitosis. Levels higher than the dilution model would suggest that cccDNA is somehow amplified following mitosis (amplification, white area), whereas levels lower than the loss model (degradation, dark grey area) would suggest other cccDNA degradation mechanisms, for example, cytokine-induced cccDNA degradation. HepG2-NTCP (top) and HepaRG-NTCP (bottom) cells were infected and harvested as per setup 1 or 2. The cccDNA decrease according to the dilution and loss models (dashed lines) were predicted using only the 0 passage (p0) time-point. Data points (connected by light lines) represent 3 independent experiments and the mean observed values for setup 1 or setup 2 are shown in solid green and red lines, respectively. cccDNA, covalently closed circular DNA; cinqPCR, cccDNA inversion quantitative PCR; dpi, days post-infection.

Results

Prediction of cccDNA levels following mitosis

We predicted the levels of cccDNA following cell mitosis given each of the 2 major hypothetical models: (i) the *cccDNA loss* model, where the cccDNA pool in an infected cell is not conveyed at all to the daughter cells after mitosis; and (ii) the *cccDNA*

dilution model, where the entire cccDNA pool is distributed amongst the daughter cells.

We assumed that each cell has an equal probability of undergoing mitosis, thereby resulting in a Poisson frequency distribution in rounds of mitosis per cell. This assumption predicts that 63.2% of cells would undergo at least 1 mitosis cycle following an average of 1 cell division of the bulk population. Thus, in the model where cccDNA is completely lost after mitosis, 36.8% of cells maintain their cccDNA. Assuming cccDNA is diluted upon mitosis and no new cccDNA is formed,[16] the cccDNA copy numbers do not change.

In both the loss and dilution models, the cell population doubles; thus, the number of cccDNA molecules per cell reduces by 50%. Thus, the loss model predicts an average net reduction to 18.4% of initial cccDNA levels per cell after each round of mitosis, whereas the dilution model predicts a reduction to 50% per round of mitosis. In both models, the predicted reduction in cccDNA is independent of the size of the cccDNA pool per cell.

HBV cccDNA levels profoundly decline following cell division, indicating complete elimination in daughter cells

We tested these predictions in 2 different HBV-susceptible cell lines, HepG2-NTCP and HepaRG-NTCP cells. After initial cccDNA establishment (3 dpi), the infected cells were serially passaged (1:2) every 3 days to induce cell mitosis. We developed 2 experimental setups (Fig. 1A): setup 1, where total cellular DNA was extracted immediately following the splitting procedure; and setup 2, where cells were cultured until 12 dpi to control for any cccDNA level changes occurring during the time course (*e.g.* via cccDNA amplification or degradation in resting cells). cccDNA molecules per cell were then precisely quantified by cinqPCR. The initial levels of cccDNA in HepG2-NTCP cells before splitting ranged between 1 and 0.5 copies per cell, similar to the levels previously described in the primary human hepatocytes of HBV-infected humanised mice.[27,28] Lower levels were observed in HepaRG-NTCP cells (on average, ~0.1 copies per cell), consistent with our previous studies.[15,16] With serial splitting, the decreases in cccDNA levels closely matched those expected from the loss model for both HepG2-NTCP (Fig. 1B) and HepaRG-NTCP (Fig. 1C) cells.

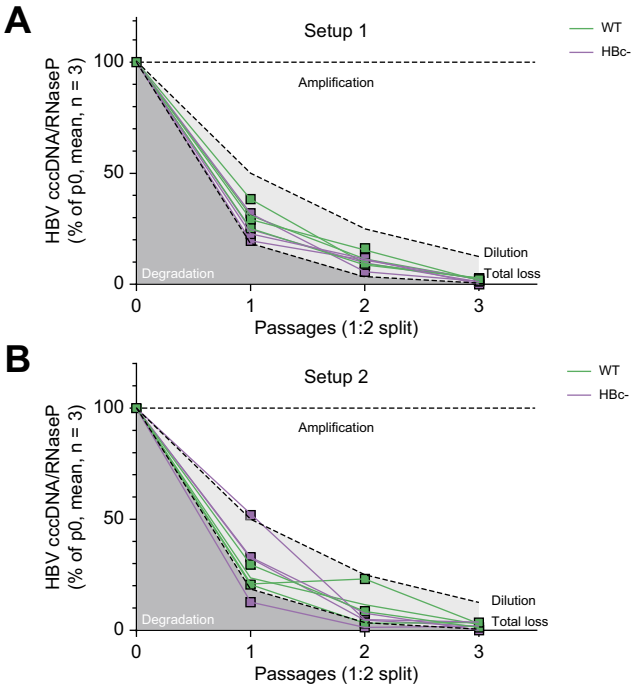

Fig. 2. Mitosis-associated cccDNA loss is unaffected by *de novo* viral replication. HepG2-NTCP cells were infected with either WT HBV (green) or replication-deficient HBV mutants containing a stop codon in the HBc ORF (purple). The infected cells were then serially split according to (A) setup 1 or (B) setup 2, as described in Fig. 2A. Data points (connected by light lines) represent 3 independent experiments, and the mean observed values are shown in solid green and purple lines for WT and HBc-deficient mutant-infected cells, respectively. cccDNA, covalently closed circular DNA; HBc, HBV core protein; ORF, open reading frame; WT, wild type.

Abrogation of HBV replication did not increase rates of cccDNA loss

In the previous experiment, we had not blocked viral replication. We tested if the mitosis-dependent reduction in cccDNA levels could be accelerated by inhibiting viral replication, as cccDNA has been assumed to be replenished by nuclear import of mature nucleocapsids in the cytosol. Such a mechanism can be impeded using a replication-deficient virus. Therefore, we investigated the post-mitotic levels of cccDNA in HepG2-NTCP cells infected with replication-deficient HBV with an early stop codon in the HBc ORF.[16] If the nuclear import pathway was indeed active, then cccDNA levels would be lower in cells infected with

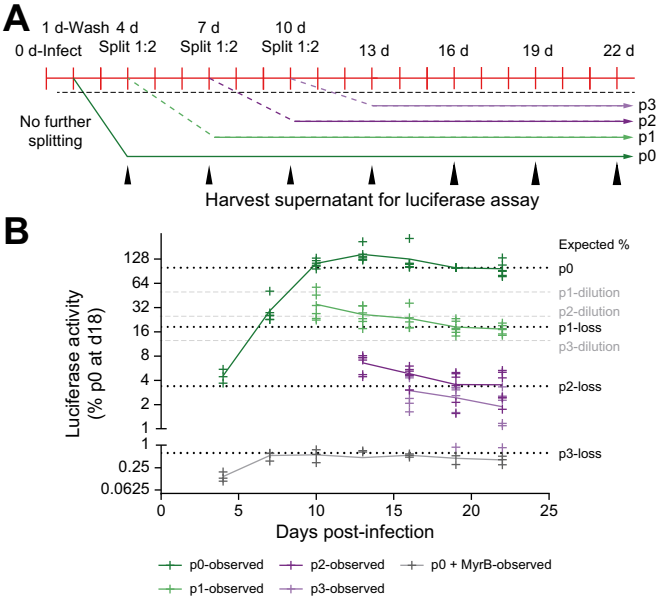

Fig. 3. The cccDNA lost with mitosis is transcriptionally active. (A) HepG2-NTCP cells infected with a Gaussia luciferase-expressing reporter HBV and serially split as per the experimental timeline. Supernatant was collected every 3 days to be measured for luciferase activity. Dashed black lines represent times where cell supernatants were not measured to allow cells to reach confluence and reach expression equilibrium. (B) Luciferase activity is plotted as a percentage of the activity at 15–18 days post-infection for each independent replicate (*y*-axis is on a log2 scale for clarity). Horizontal lines represent the reduction expected from the dilution (dashed grey lines) or complete loss (dotted black lines) models. The mean activity of each serial time point taken from the un-split (dark green) and those split once (light green), twice (dark purple), and thrice (light purple) are shown in thick dashed lines (individual observations in crosses, n = 6 per time point). Luciferase activity detected in the supernatant of un-split cells pretreated with viral entry inhibitor Myrcludex B (negative control) is presented as grey data points. cccDNA, covalently closed circular DNA.

HBc-deficient mutants compared with WT HBV. This experimental setup also tests the contribution of *de novo* HBV spread in the culture to cccDNA levels (although this is not expected to occur in cell culture as shown previously[16]).

We observed no difference in the rate of cccDNA reduction during serial rounds of mitosis between cells infected with HBc-deficient HBV or WT virus in setup 1 or 2, as described in Fig. 1 (Fig. 2). We conclude that HBV spread, replication, or cytoplasmic mature nucleocapsids do not play significant roles in cccDNA levels after mitosis of HBV-infected daughter cells. Essentially, these results suggest that treatment with direct acting antiviral therapies (such as nucleoside analogues and capsid inhibitors) would not directly affect cccDNA loss by this mechanism. Moreover, this information allows us to use a replication-defective, virus to further investigate cccDNA loss, knowing that the lack of virus replication would not impact these dynamics.

Expression from cccDNA declines at a rate consistent with cccDNA loss with mitosis

We determined if protein expression from cccDNA also declined at the same rate as cccDNA copy number. We found that the detection of secreted viral antigens (HBeAg and HBsAg) by ELISA was insufficiently sensitive to precisely and accurately determine the relatively low levels of secretion after several rounds of mitosis (data not shown). We instead used rHBV-TTR-GLuc in place of the HBsAg ORF to infect HepG2-NTCP cells and used a serial-splitting experimental design similar to setup 2 described above (Fig. 3A). Luciferase activity can be detected with much higher sensitivity compared with HBV antigens and was measured in the supernatant of infected cells 6 days following passage (thereby allowing cells to divide and then secrete sufficient luciferase into the supernatant).

Reduction of luciferase activity paralleled the reduction of cccDNA levels expected by the loss model (i.e. a reduction of ~5-fold with each successive split) compared with the dilution model (2-fold reduction per split), except for cells after the third passage where high variation (caused by low signal) prevented clear observation of signal reduction (Fig 3B). Luciferase activity was relatively stable after reaching a plateau, suggesting there were no fluctuations caused by temporary epigenetic changes of transgene expression after cellular mitosis. Luciferase activity of negative controls pretreated with virus entry inhibitor Myrcludex B never exceeded 0.8% at any time point, indicating that all detected signals were caused by *bona fide* HBV infection. In conclusion, we show that the HBV cccDNA that is lost with mitosis is transcriptionally active and its loss parallels the reduction in viral protein expression.

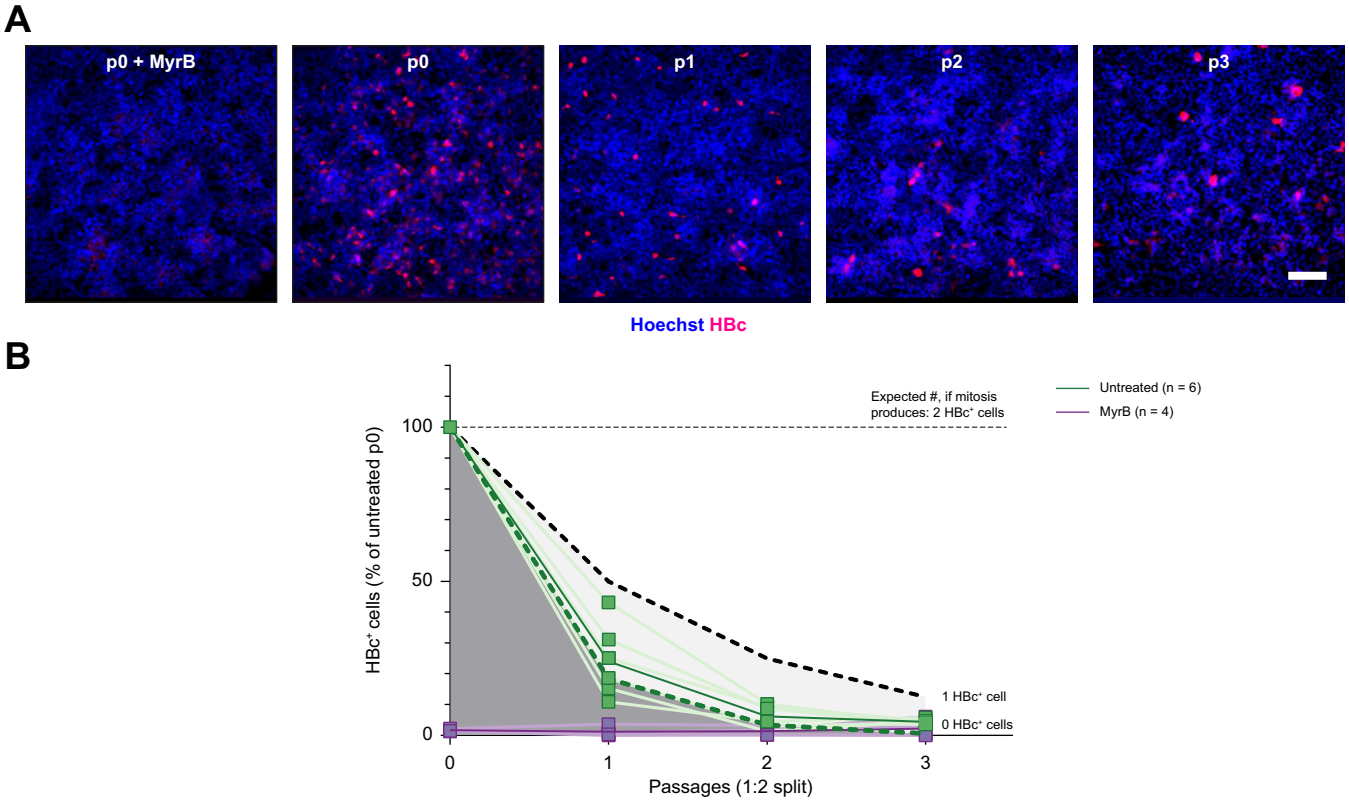

Fig. 4. Number of HBc-positive cells decreases with serial passaging consistent with cccDNA loss with mitosis. (A) HBV-infected HepG2-NTCP cells were treated as per setup 2 (Fig. 2A), fixed at 12 days post-infection, and visualised by fluorescence microscopy (HBc in red, Hoechst staining for cell nuclei in blue). Scale bar = 100 μm. MyrB = cells pretreated with HBV entry inhibitor Myrcludex B as a negative control. (B) A marked decrease in HBc-positive cells was observed with each additional split (green), highly consistent with the loss of HBV cccDNA in daughter cells of infected hepatocytes. Dashed lines represent the number of cells expected per split if 1 or 2 daughter cells (dilution model) or 0 daughter cells (complete loss model) were HBc-positive following mitosis. The percentage of HBc-positive cells was calculated by dividing the number of HBc-positive cells by the number of nuclei in 5 randomly picked fields of view. Few RFP-positive cells were observed in those pretreated with the HBV entry inhibitor Myrcludex B (purple), showing *bona fide* infection had occurred. cccDNA, covalently closed circular DNA; HBc, HBV core protein.

HBV-positive cells were rarely clustered after mitosis and decreased at rates consistent with complete cccDNA loss

We next visualised HBV-infected cells from setup 2 on a single-cell level using immunofluorescence for HBc. HepG2-NTCPs showed a marked reduction in HBc-positive cell numbers after cell mitosis (Fig. 4A). The HBc-positive cells after mitosis induction present as individual cells (likely infected cells that have not undergone mitosis), which is consistent with the loss model. On the contrary, the dilution model would predict some cluster formation of 2 or more adjacent HBc-positive cells. Identical patterns were seen in HepaRG-NTCP cells (Fig. S1). The number of HBc-positive cells (Fig. 4B) at each passage more closely matched mathematical models where 2 HBc-negative daughter cells result from mitosis (complete loss), compared with those where either 1 or 2 HBc-positive daughter cells results from mitosis of infected cells (dilution model). Together, these data provide further support for the complete loss model.

Live cell imaging showed that daughter cells of HBV-infected hepatocytes are viable and express no new viral antigens after mitosis

Finally, we determined the fate of individual HBV-infected cells that undergo mitosis, specifically whether they undergo cell death or if they do indeed produce 2 uninfected daughter cells. To track living HBV-infected cells, we infected HepG2-NTCP cells with tRFP-HBV. Given the long half-life of tRFP mRNA (~10 h[29]) and protein (~40 h[30]), we could track by live imaging the daughter cells of HBV-infected cells for a short time after cell mitosis.

HepG2-NTCP cells infected with tRFP-HBV were seeded in DMSO-free DMEM into chamber slides at ~100,000 cells per cm^2 (about the concentration of a 1:1.5 split in comparison with previous experiments), allowing us to observe areas of high confluence (and therefore low mitosis) as well as low confluence/high mitosis. Live cell imaging was carried out over 36 h (Fig. 5A). In areas of low confluence, we observed multiple instances of tRFP-positive cells undergoing mitosis, producing 2 living daughter cells containing tRFP (Fig. 5B). In high-confluence areas, tRFP expression was stable in non-dividing cells. Thus, division of HBV-infected cells does not induce cell death of daughter cells.

We then tested if new tRFP was being expressed in the daughter cells by photo-bleaching all existing tRFP. After exposure to 560/40-nm light for 10 min, cells were allowed to recover for 5 h and re-imaged. All tRFP-positive cells that had undergone mitosis in low-confluence areas had lost positive signals, whereas the cells that did not undergo mitosis (in high-confluence areas and the rare cells in low-confluence areas) maintained positivity for tRFP (Fig. 5B). This suggests that HBV-infected cells lose cccDNA directly after mitosis.

Discussion

In this study, we provide mathematical modelling and multiple lines of evidence showing that cccDNA is not propagated to daughter cells after mitosis in *in vitro* models of HBV infection. Reduction of cccDNA levels in HepG2-NTCP (a hepatoma cell line) and HepaRG-NTCP (a hepatocyte-like cell line differentiated

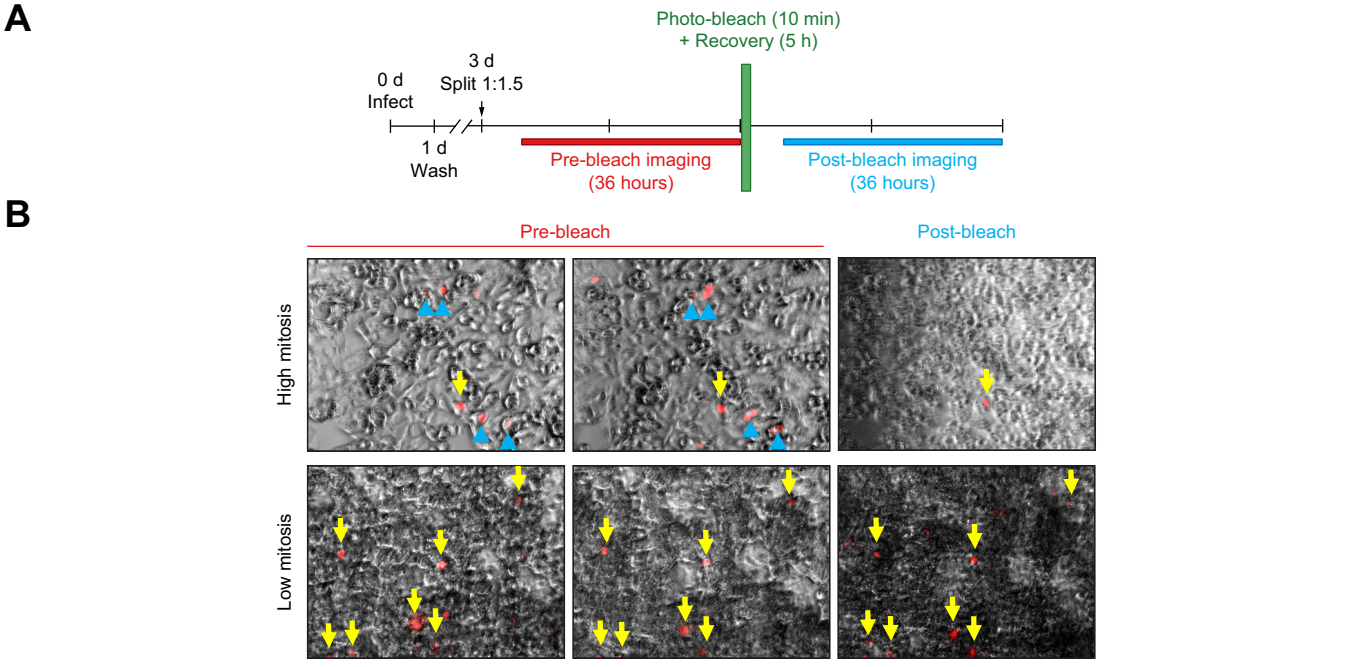

Fig. 5. Live cell imaging shows that HBV-infected cells that undergo mitosis produce viable daughter cells free of transcriptionally active cccDNA. (A) HepG2-NTCP cells infected with a tRFP-expressing reporter HBV and reseeded at a lower density (equivalent to a 1:1.5 split) in a chamber slide. After being allowed to reattach to the slide bottom for 12 h, the cells were live-imaged in a humidity-, heat-, and CO_2-controlled chamber (1 capture every 15 min for 36 h). Cells were then photo-bleached with 10-min exposure of 560/40-nm laser light, and the cells were allowed to recover for 5 h to limit excess photo-toxicity associated with image acquisition. Live acquisition was then continued for another 36 h in the post-bleaching stage. Acquisition was measured at 40× with excitation filters at 560/40-nm and emission filters at 630/75-nm for RFP fluorescence and white light for phase contrast. (B) Stills from live imaging in prebleach (left and centre panels) and post-bleach (right panel) time-points in fields of view with low confluence (high mitosis, top row) or high confluence (low mitosis, bottom row). RFP-positive cells that did not undergo mitosis in the prebleach period are marked with a yellow arrow, whereas cells in which mitosis was observed are marked with a blue triangle. No RFP-positive cells that underwent mitosis maintained positive staining after bleaching. cccDNA, covalently closed circular DNA.

from bipotent progenitor cells) suggests that cccDNA is lost after mitosis of an infected cell. Although some of our results are based on mathematical modelling and therefore sensitive to assumptions (*e.g.* that HBV-infected cells enter mitosis at the same rate as uninfected cells), our live cell imaging experiments directly showed on a single-cell level that cccDNA is lost in cells undergoing mitosis. Thus, this non-cytolytic pathway for cccDNA clearance via cell mitosis is highly efficient.

Some reports have suggested partial maintenance of cccDNA molecules in daughter cells after mitosis.[4,10,13,14] These studies have generally used non-human model systems in which higher numbers of cccDNA per cell are generated: these include woodchuck[4] and duck[10] models and HepAD38 cells[13] in which viral replication and subsequent cccDNA formation is controlled by tetracycline. Moreover, nuclear import of mature nucleocapsids is a highly active feature in animal and overexpression models, but this route appears to contribute minimally to the cccDNA levels in human HBV infection models *in vitro*[16] and in humanised mice.[31] Future work is needed to confirm that these dynamics extend to the HBV-infected liver in humans.

Another difference to previous studies is the extent of mitosis induced: our experiments focused on only a few rounds of mitosis, whereas others performed splitting at higher dilutions and measured over longer periods – up to 30 weeks – after infection. For example, a previous report studied immune deficient urokinase-type plasminogen activator/severe combined immunodeficiency (uPA/SCID)/beige mice implanted with HBV-infected hepatocytes, which repopulate the mouse liver after multiple rounds of mitosis.[8] In this system and consistent with the present data, rare non-dividing cells were found to maintain infection, whereas virus was eliminated in the bulk repopulated culture.

These data suggest heterogeneity in the host-cell population, where slow-growing or non-dividing cells may effectively act as viral reservoirs (consistent with previously published mathematical models[32]). In agreement with this hypothesis, previous studies have shown non-random hepatocyte repopulation with selective clonal expansion being observed in people with chronic hepatitis B and in animal models of hepatitis B[33–37] and other liver injuries.[38] The effect of these heterogeneous cellular behaviours suggests that deciphering which route plays the major role for cccDNA persistence may identify a more efficient mechanism to clear cccDNA.

The results described here also impact the interpretation of future studies of cccDNA decay and therapeutic reduction. For example, our work suggests that a 2-fold reduction in cccDNA per cell would result from a cumulative turnover of ~35% of the cells in a culture. Thus, even slight levels of cytotoxicity or cell mitosis (particularly over long periods of culture) could dramatically reduce cccDNA levels. We therefore recommend that studies of investigational drugs or therapeutic approaches to specifically reduce cccDNA should determine carefully if the induction of mitosis contributes to the mechanism of action.

In contrast, our work (in addition to other concordant studies) justifies a focus on therapeutic approaches that induce liver turnover to efficiently clear high levels of cccDNA. Indeed, cell mitosis has been described through mathematical modelling as the major driver of cccDNA loss in acute HBV infections of both animal models and humans.[7,39,40] Potential therapeutic strategies include immuno-modulators to induce liver turnover, although these would require considered application to avoid hepatic decompensation or carcinogenic risk. A targeted agent that induces the mitosis of specifically HBV-infected cells could overcome these risks. This theoretical agent would be a part of a combination of therapies to effect a cure: new infection events need to be inhibited to prevent *de novo* cccDNA formation, which can be achieved by concomitant treatment with viral entry inhibitors, capsid inhibitors, and/or nucleot(s)ide analogues.

The exact fate of cccDNA after cell mitosis remains a mystery but is presumably degraded such that they cannot be detected by cinqPCR. In other contexts, circular host DNA (*e.g.* extrachromosomal circular DNA) can be incorporated into micronuclei[41] where it can be degraded by host DNases (*e.g.* TREX1[42]). In addition, cytoplasmic DNA is detected by cyclic GMP-AMP synthase,[43] which induces DNA degradation by cellular autophagy.[44] It is feasible that cytoplasmic HBV cccDNA (after mitosis) could be degraded through similar routes. To show this would require technically challenging assays for tracking these molecules post-mitosis (*e.g.* fluorescence *in situ* hybridisation specific enough to only detect cccDNA) and is currently beyond our capabilities.

In summary, we have uncovered a fundamental aspect of cccDNA dynamics that impacts the understanding of the viral persistence driving chronic HBV infections. Given the strong evidence that mitosis of infected hepatocytes results in uninfected daughter cells, greater focus should be applied to determine exactly how cccDNA can persist despite marked liver turnover during hepatic inflammatory flares. The answer to this ongoing problem may hold the key to inducing a complete cure of chronic hepatitis B.

Abbreviations

cccDNA, covalently closed circular DNA; cinqPCR, cccDNA inversion quantitative PCR; ddPCR, digital droplet PCR; dpi, days post-infection; Gluc, Gaussia luciferase; HBc, HBV core protein; ORF, open reading frame; rHBV, reporter HBV; TTR, transthyretin; tRFP, turbo-RFP; WT, wild type.

Financial support

This work received funding from the following: the German Centre for Infection Research (DZIF) TTU Hepatitis Projects 5.807 and 5.704 (TT and SU); the Deutsche Forschungsgemeinschaft (DFG, German Research Foundation), Project Number 240245660; SFB 1129 (BZ and SU) and – Project Number 272983813 – TRR179 (TP 15) (SU); the Australian Centre for HIV and Hepatitis Virology Research (TT); the Australian National Health and Medical Research Council Ideas Grant APP2002565 (TT and MD), Program Grants APP1053206 and APP1149976 and Project Grants APP1107178 and APP1108422 (JG); and the Robert W. Storr Bequest to the Sydney Medical Foundation (JG). Microscopy was performed at the Westmead Scientific Platforms, which are supported by the Westmead Research Hub, the Cancer Institute New South Wales, the National Health and Medical Research Council, and the Ian Potter Foundation.

Conflicts of interest

SU is co-applicant and co-inventor on patents protecting HBV preS-derived lipopeptides (Myrcludex B) for the use of HBV/HDV entry inhibitors. UP is a co-founder and shareholder of SCG Cell Therapy. The other authors in this study declare no relevant competing interests.

Please refer to the accompanying ICMJE disclosure forms for further details.

Authors' contributions

Conceived the concept of the project: TT. Designed the experiments: TT. Carried out the experiments: TT, HZ, SC, VH. Analysed the data: TT. Generated figures: TT. Wrote the manuscript: TT. Designed and carried out the HBc-deficient mutant experiments: BZ. Assisted in writing the manuscript: BZ, HZ, SC, VH, UP. Assisted in the experimental design: HZ, SC, VH, JW. Generated the reporter viruses: JW. Contributed to writing the manuscript: JW, MD, JG, SU. Provided funding for JW: UP. Provided funding for TT, VH, and parts of the project: MD and JG. Provided funding for TT, BZ, and parts of the project: SU. Contributed intellectual input on experimental design: SU.

Data availability statement

All data generated or analysed during this study are included in this published article (and its Supporting information files).

Acknowledgements

We acknowledge Drs Yi Ni and Florian A. Lempp for reagents (cell lines and HBV inoculum) and Lisa Walter, Anja Rippert, Franziska Schlund, Dr Christa Kuhn, and Westmead Research Hub for their technical assistance. We are grateful to Dr Zhenfeng Zhang for helpful discussions, Miriam Kleinig for proofreading, and Prof. Dr Ralf Bartenschlager for continuous support.

Supplementary data

Supplementary data to this article can be found online at https://doi.org/10.1016/j.jhepr.2022.100514.

References

Author names in bold designate shared co-first authorship

[1] Stanaway JD, Flaxman AD, Naghavi M, Fitzmaurice C, Vos T, Abubakar I, et al. The global burden of viral hepatitis from 1990 to 2013: findings from the Global Burden of Disease Study 2013. Lancet 2016;388:1081–1088.
[2] Tu T, Block JM, Wang S, Cohen C, Douglas MW. The lived experience of chronic hepatitis B: a broader view of its impacts and why we need a cure. Viruses 2020;12:515.
[3] Moraleda G, Saputelli J, Aldrich CE, Averett D, Condreay L, Mason WS. Lack of effect of antiviral therapy in nondividing hepatocyte cultures on the closed circular DNA of woodchuck hepatitis virus. J Virol 1997;71:9392–9399.
[4] Dandri M, Burda MR, Will H, Petersen J. Increased hepatocyte turnover and inhibition of woodchuck hepatitis B virus replication by adefovir in vitro do not lead to reduction of the closed circular DNA. Hepatology 2000;32:139–146.
[5] Lucifora J, Xia Y, Reisinger F, Zhang K, Stadler D, Cheng X, et al. Specific and nonhepatotoxic degradation of nuclear hepatitis B virus cccDNA. Science 2014;343:1221–1228.
[6] Guidotti LG, Rochford R, Chung J, Shapiro M, Purcell R, Chisari FV. Viral clearance without destruction of infected cells during acute HBV infection. Science 1999;284:825–829.
[7] Murray JM, Wieland SF, Purcell RH, Chisari FV. Dynamics of hepatitis B virus clearance in chimpanzees. Proc Natl Acad Sci U S A 2005;102:17780–17785.
[8] Allweiss L, Volz T, Giersch K, Kah J, Raffa G, Petersen J, et al. Proliferation of primary human hepatocytes and prevention of hepatitis B virus reinfection efficiently deplete nuclear cccDNA in vivo. Gut 2018;67:542–552.
[9] Lok AS, Zoulim F, Dusheiko G, Ghany MG. Hepatitis B cure: from discovery to regulatory approval. J Hepatol 2017;67:847–861.
[10] Reaiche-Miller GY, Thorpe M, Low HC, Qiao Q, Scougall CA, Mason WS, et al. Duck hepatitis B virus covalently closed circular DNA appears to survive hepatocyte mitosis in the growing liver. Virology 2013;446:357–364.
[11] Murray JM, Goyal A. In silico single cell dynamics of hepatitis B virus infection and clearance. J Theor Biol 2015;366:91–102.
[12] Lutgehetmann M, Volz T, Köpke A, Broja T, Tigges E, Lohse AW, et al. In vivo proliferation of hepadnavirus-infected hepatocytes induces loss of covalently closed circular DNA in mice. Hepatology 2010;52:16–24.
[13] Li M, Sohn JA, Seeger C. Distribution of hepatitis B virus nuclear DNA. J Virol 2018;92. e01391-17.
[14] Zhu Y, Yamamoto T, Cullen J, Saputelli J, Aldrich CE, Miller DS, et al. Kinetics of hepadnavirus loss from the liver during inhibition of viral DNA synthesis. J Virol 2001;75:311–322.
[15] Tu T, Zehnder B, Qu B, Ni Y, Main N, Allweiss L, et al. A novel method to precisely quantify Hepatitis B Virus covalently closed circular (ccc)DNA formation and maintenance. Antivir Res 2020;181:104865.
[16] **Tu T**, **Zehnder B**, Qu B, Urban S. De novo synthesis of Hepatitis B virus nucleocapsids is dispensable for the maintenance and transcriptional regulation of cccDNA. JHEP Rep 2020;3:100195.
[17] Ladner SK, Otto MJ, Barker CS, Zaifert K, Wang GH, Guo JT, et al. Inducible expression of human hepatitis B virus (HBV) in stably transfected hepatoblastoma cells: a novel system for screening potential inhibitors of HBV replication. Antimicrob Agents Chemother 1997;41:1715–1720.
[18] Lempp FA, Mutz P, Lipps C, Wirth D, Bartenschlager R, Urban S. Evidence that hepatitis B virus replication in mouse cells is limited by the lack of a host cell dependency factor. J Hepatol 2016;64:556–564.
[19] Wing PA, Davenne T, Wettengel J, Lai AG, Zhuang X, Chakraborty A, et al. A dual role for SAMHD1 in regulating HBV cccDNA and RT-dependent particle genesis. Life Sci Alliance 2019;2:e201900355.
[20] Wettengel JM, Linden B, Esser K, Laue M, Burwitz BJ, Protzer U. Rapid and robust continuous purification of high-titer hepatitis B Virus for in vitro and in vivo applications. Viruses 2021;13:1503.
[21] Gripon P, Rumin S, Urban S, Le Seyec J, Glaise D, Cannie I, et al. Infection of a human hepatoma cell line by hepatitis B virus. Proc Natl Acad Sci U S A 2002;99:15655–15660.
[22] Ni Y, Lempp FA, Mehrle S, Nkongolo S, Kaufman C, Fälth M, et al. Hepatitis B and D viruses exploit sodium taurocholate co-transporting polypeptide for species-specific entry into hepatocytes. Gastroenterology 2014;146:1070–1083.
[23] Schulze A, Mills K, Weiss TS, Urban S. Hepatocyte polarization is essential for the productive entry of the hepatitis B virus. Hepatology 2012;55:373–383.
[24] Schneider CA, Rasband WS, Eliceiri KW. NIH Image to ImageJ: 25 years of image analysis. Nat Methods 2012;9:671–675.
[25] Berg S, Kutra D, Kroeger T, Straehle CN, Kausler BX, Haubold C, et al. ilastik: interactive machine learning for (bio)image analysis. Nat Methods 2019;16:1226–1232.
[26] Zehnder B, Urban S, Tu T. A sensitive and specific PCR-based assay to quantify hepatitis B virus covalently closed circular (ccc) DNA while preserving cellular DNA. Bio Protoc 2021;11:e3986.
[27] Allweiss L, Volz T, Lütgehetmann M, Giersch K, Bornscheuer T, Lohse AW, et al. Immune cell responses are not required to induce substantial hepatitis B virus antigen decline during pegylated interferon-alpha administration. J Hepatol 2014;60:500–507.
[28] Lutgehetmann M, Bornscheuer T, Volz T, Allweiss L, Bockmann JH, Pollok JM, et al. Hepatitis B virus limits response of human hepatocytes to interferon-alpha in chimeric mice. Gastroenterology 2011;140:2074–2083.
[29] Yang E, van Nimwegen E, Zavolan M, Rajewsky N, Schroeder M, Magnasco M, et al. Decay rates of human mRNAs: correlation with functional characteristics and sequence attributes. Genome Res 2003;13:1863–1872.
[30] Shaner NC, Lin MZ, McKeown MR, Steinbach PA, Hazelwood KL, Davidson MW, et al. Improving the photostability of bright monomeric orange and red fluorescent proteins. Nat Methods 2008;5:545–551.
[31] Volz T, Allweiss L, Ben MM, Warlich M, Lohse AW, Pollok JM, et al. The entry inhibitor Myrcludex-B efficiently blocks intrahepatic virus spreading in humanized mice previously infected with hepatitis B virus. J Hepatol 2013;58:861–867.
[32] Lythgoe KA, Lumley SF, Pellis L, McKeating JA, Matthews PC. Estimating hepatitis B virus cccDNA persistence in chronic infection. Virus Evol 2021;7. veaa063.
[33] Mason WS, Gill US, Litwin S, Zhou Y, Peri S, Pop O, et al. HBV DNA integration and clonal hepatocyte expansion in chronic hepatitis b patients considered immune tolerant. Gastroenterology 2016;151:986–988.e984.
[34] Mason WS, Jilbert AR, Summers J. Clonal expansion of hepatocytes during chronic woodchuck hepatitis virus infection. Proc Natl Acad Sci U S A 2005;102:1139–1144.
[35] Mason WS, Liu C, Aldrich CE, Litwin S, Yeh MM. Clonal expansion of normal-appearing human hepatocytes during chronic hepatitis B virus infection. J Virol 2010;84:8308–8315.
[36] Mason WS, Low HC, Xu C, Aldrich CE, Scougall CA, Grosse A, et al. Detection of clonally expanded hepatocytes in chimpanzees with chronic hepatitis B virus infection. J Virol 2009;83:8396–8408.

[37] Tu T, Mason WS, Clouston AD, Shackel NA, McCaughan GW, Yeh MM, et al. Clonal expansion of hepatocytes with a selective advantage occurs during all stages of chronic hepatitis B virus infection. J Viral Hepat 2015;22:737–753.
[38] Wei Y, Wang YG, Jia Y, Li L, Yoon J, Zhang S, et al. Liver homeostasis is maintained by midlobular zone 2 hepatocytes. Science 2021;371: eabb1625.
[39] Goyal A, Ribeiro RM, Perelson AS. The role of infected cell proliferation in the clearance of acute HBV infection in humans. Viruses 2017;9:350.
[40] Whalley SA, Murray JM, Brown D, Webster GJ, Emery VC, Dusheiko GM, et al. Kinetics of acute hepatitis B virus infection in humans. J Exp Med 2001;193:847–854.
[41] Von Hoff DD, McGill JR, Forseth BJ, Davidson KK, Bradley TP, Van Devanter DR, et al. Elimination of extrachromosomally amplified MYC genes from human tumor cells reduces their tumorigenicity. Proc Natl Acad Sci U S A 1992;89:8165–8169.
[42] Mohr L, Toufektchan E, von Morgen P, Chu K, Kapoor A, Maciejowski J. ER-directed TREX1 limits cGAS activation at micronuclei. Mol Cell 2021;81:724–728.e729.
[43] Sun L, Wu J, Du F, Chen X, Chen ZJ. Cyclic GMP-AMP synthase is a cytosolic DNA sensor that activates the type I interferon pathway. Science 2013;339:786–791.
[44] Gui X, Yang H, Li T, Tan X, Shi P, Li M, et al. Autophagy induction via STING trafficking is a primordial function of the cGAS pathway. Nature 2019;567:262–266.